Surface & Coatings Technology 258 (2014) 549–556

Contents lists available at ScienceDirect

Surface & Coatings Technology

journal homepage: www.elsevier.com/locate/surfcoat

Metal surface layers after pulsed electron beam treatment

Renate Fetzer *, Georg Mueller, Wladimir An, Alfons Weisenburger

Karlsruhe Institute of Technology, PO Box 3640, Karlsruhe 76021, Germany

ARTICLE INFO

Article history:
Received 14 May 2014
Accepted in revised form 16 August 2014
Available online 25 August 2014

Keywords:
Pulsed electron beam
Surface modification
Melt layer dynamics

ABSTRACT

Irradiation of metal targets with intense pulsed electron beams leads to rapid melting and solidification of the target surface layers. For beams generated by the GESA facility with 120 kV acceleration voltage, 20–80 J/cm^2 beam energy density, and 20–50 μs pulse duration, the induced changes in material properties are accompanied by the evolution of a topographical pattern on the target surface, typically tens of micrometers in height and hundreds of micrometers laterally. In this work, GESA-modified surface layers of stainless steel, copper, and aluminum alloy targets are characterized by a post-treatment study. Larger surface roughness is found for treatment with an electron beam of higher energy density. Similarly, the roughness amplitude increases for the repetitive application of high energy density pulses (60–80 J/cm^2, 40–50 μs). Several shorter pulses with lower energy density (~30 J/cm^2, 25–30 μs) lead to a coarsening of the surface features. The target material inhomogeneity and the aspect of the melt front are investigated by cross-sectional analysis. Material homogenization is observed in the melted surface layer. Straight melt fronts are found for stainless steel, whereas aluminum alloy shows non-uniform melting. Based on the experimental findings, different processes and their influence on the surface layer dynamics during the melted stage are discussed. These include intense evaporation and dissolution of inclusions into the surrounding melt material.

1. Introduction

Pulsed electron beam treatment of metal targets has gained technological relevance in the past decades due to improved surface properties such as hardness, wear resistance, corrosion resistance, and antimicrobial properties [1–4]. For short pulses with large enough energy densities, rapid heating and melting of the surface layer is achieved, followed by fast cooling and solidification into a modified layer. In most cases, surface modification is accompanied by the development of a topographical pattern on the target surface.

Craters, 10–100 μm in diameter, are typically observed on metal targets treated with beams of 10–40 keV electron energy, 1–3 μs pulse duration, and 2–10 J/cm^2 energy density [5,6]. It is believed that they are caused by eruptions due to local sub-surface overheating of chemical inclusions and precipitates [7,8]. Application of several pulses in this case leads to selective surface purification and smoothening of the target surfaces [5–7]. Significant evaporation of target material during pulsed electron beam treatment is found to cause a wavy surface topography, observed for instance on AZ31 Mg alloy [9] and NiTi alloy targets [10]. Longer pulses (~20 μs) and higher energy densities (~20 J/cm^2) induce melting of surface layers with larger thickness and longer lifetime, which allows surface tension to relax the free liquid surface and hydrodynamic instabilities to become relevant. Depending on the target material, either a relatively smooth target surface is achieved (in case of sulfur-free Fe) or an anomalous surface tension (positive temperature derivative) due to the presence of sulfur in carbon and stainless steel targets leads to a surface pattern similar to that of dewetting [11].

Intense pulsed electron beams with 120 keV electron energy, 1–2 MW/cm^2 beam power density and 20–50 μs pulse duration (20–80 J/cm^2 beam energy density) as generated by the GESA facility cause the development of a topographical pattern on the target surface with tens of micrometers in height and hundreds of micrometers on the lateral scale. In order to gain knowledge about the interaction of electron beams, with parameters typical for GESA, and metal targets, various fast in situ diagnostic tools were set up and applied in recent years [12–14]. From time- and space-resolved surface specular reflectivity measurements, the onset of melting and solidification was determined [12]. The vapor and plasma phase in the vicinity of the target surface was studied [13]. Impact ionization by beam electrons was found to result in a low-density low-temperature target plasma, excluding electric fields in the plasma sheath to be responsible for the growth of the surface features. High-resolution schlieren imaging and a stroboscopic imaging technique allowed the detailed observation of surface irregularities during treatment [14]. Around the onset of melting, bubbles and micro-irregularities were found at the target surface. In addition, splashing of droplets was observed for aluminum alloy targets around beam termination. So far, however, no systematic study exists that relates the electron beam parameters and the sequence of their application with the characteristic topographical pattern found on the target surfaces after the treatment. This relation is investigated in the present

* Corresponding author. Tel.: +49 721 608 24263; fax: +49 721 608 22256.
E-mail address: renate.fetzer@kit.edu (R. Fetzer).

http://dx.doi.org/10.1016/j.surfcoat.2014.08.039
0257-8972/

post-treatment study for stainless steel, copper, and aluminum alloy targets, complemented by further characterization of the GESA-modified surface layers.

2. Methods

Intense large-area electron beams are generated and directed toward the metal target in the GESA I facility [15]. A high-voltage pulse (120 kV) is supplied to a triode consisting of an explosive emission cathode, a grid, and a ring-shaped anode. The electrons are homogeneously emitted from the cathode, accelerated toward the anode and focused by a guiding magnetic field toward the target. At the metal target, a Gaussian beam profile is found, with a diameter of ca. 6 cm and a power density of 1–2 MW/cm^2 in the beam center. The total energy density deposited in the central area can be adjusted to values between 10 and 80 J/cm^2 by setting the pulse duration within the range 15–50 μs. Triode and target are placed in a vacuum chamber (2–5 mPa).

Targets are 15 × 15 mm^2 pieces cut from 1.5 to 2 mm thick sheet metal. Materials used in this study are stainless steel (SS 304), copper (Cu), and aluminum alloy (AlMg3, 2.5–3.6 wt% Mg). Prior to mounting the targets in the GESA treatment chamber, their surfaces were grinded with 1200-grit abrasive (root mean square surface roughness Sq = 0.2–0.3 μm) and cleaned with ethanol. Weighing of the samples prior to and after the electron beam treatment allowed information about the total material loss. Normalized by the sample surface area, the lost mass per unit area was obtained. Because the samples are much smaller than the beam diameter, a uniform distribution of the mass loss over the target surface was assumed. The topography of the targets was imaged with a non-contact white light profilometer (μscan by NanoFocus) based on chromatic aberration, with a lateral resolution of 4 μm. From the profilometer images, the root mean square surface roughness Sq of the targets was determined. Cross sections were cut from selected samples, embedded in resin, grinded, and polished. After a metallographic etch, the cross sections were analyzed with optical microscopy and the thicknesses of the melted layers were obtained. The material inhomogeneity of the treated surface layer was investigated by scanning electron microscopy (SEM) including energy dispersive X-ray (EDX) analysis.

3. Target topography

3.1. Influence of target material

Typical profilometer images [13,14] of various targets after treatment with an electron beam of energy density 56 ± 2 J/cm^2 are shown in Fig. 1. Note that the images were obtained in the center of the beam footprint, where also the energy density is taken. As clearly seen, the topographical pattern depends on the target material. On stainless steel and copper, a more or less isotropic pattern of quite regular ripples evolves on the surface, the root mean square roughness Sq and typical wavelength λ of which are, respectively, Sq = 2.7 μm and λ ~540 μm for SS, and Sq = 3.9 μm and λ ~260 μm for Cu. Compared to these materials, the Al alloy shows a rather irregular pattern with a much larger roughness of Sq = 11.9 μm.

When using the same target material, the surface roughness generally increases with the heat load deposited by the beam, an example for SS is given in Fig. 2. A summary of surface roughness data obtained on various samples of SS, Cu, and Al alloy after treatment with a single GESA pulse is shown in Fig. 3. Each data point represents the roughness of one sample measured over an area of 4 × 4 mm^2 in the center of the beam footprint. Note that error bars (originating from variation of the position of the measurement) of individual data points are omitted because the scatter between different samples is much larger than the uncertainties within each target. Despite the large scatter, a general trend of increasing roughness for increasing heat load is obtained for Al alloy and Cu. The substantial scatter does not allow any conclusion on a possible saturation or even decrease of the roughness for very high energy loads. Clearly, the highest surface roughness is found on Al alloy.

Fig. 4a shows the total target material mass loss per surface area caused by the pulsed electron beam treatment in the beam center [14]. The data of Al alloy and SS fall on each other, while the Cu data stay slightly below. The data of lost mass are recalculated to obtain the thickness of the lost surface layer, see Fig. 4b. Al alloy targets clearly experience the highest loss of material in terms of thickness, followed by stainless steel. Cu shows the thinnest layer of lost material. For all materials, a beam energy density threshold exists, below which material loss is lower than the sensitivity of the weight measurement (~20 J/cm^2 for Al alloy, ~30 J/cm^2 for SS, and ~55 J/cm^2 for Cu).

In Fig. 5, the melting depths are summarized for SS, Cu, and Al alloy at various beam energy densities [14]. Solid symbols represent the values as measured optically from cross-sectional analysis (see Section 4.2.) whereas open symbols denote the overall melt depths including the thickness of lost material. The error bars indicate the variance of the melt layer thickness within each cross section. As expected, the melt depth increases for increasing deposited energy density. Stainless steel targets exhibit the thinnest melted layers, followed by Cu. Al targets show the highest melt layer thicknesses.

3.2. Repetitive treatment

So far, only freshly prepared targets treated by a single pulse were studied. The question arises whether repetitive treatment results in an accumulation of surface features or in a saturation or even decrease of surface roughness.

Repetitive treatment of stainless steel and aluminum alloy targets was investigated for three different cases, (i) consecutive high energy density pulses of about 60–80 J/cm^2 per pulse, denoted by 'H'; (ii) consecutive low energy density pulses with 29–33 J/cm^2 each, denoted by 'L'; and (iii) one high energy density pulse (H) followed by consecutive low energy density pulses (L). In each case, the sample was kept inside the evacuated treatment chamber between pulses, thus avoiding surface oxidation and contamination. In Figs. 6 and 7, respectively, the

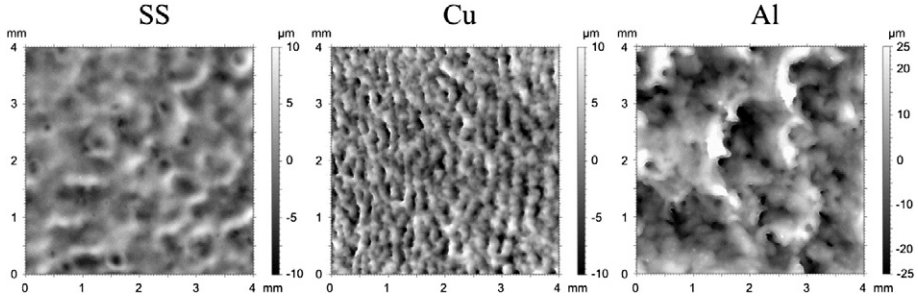

Fig. 1. Profilometer images (4 × 4 mm^2) of stainless steel, copper, and aluminum alloy after treatment with a pulsed electron beam of energy density 56 ± 2 J/cm^2. The height range is 20 μm for SS and Cu, and 50 μm for Al.